International Journal of Research in Medical Sciences
Ghasi RG. Int J Res Med Sci. 2019 Jan;7(1):77-84
www.msjonline.org
pISSN 2320-6071 | eISSN 2320-6012
DOI: http://dx.doi.org/10.18203/2320-6012.ijrms20185096

Original Research Article

Decoding neonatal chest radiographic patterns of disease: retrospective analysis from a tertiary care hospital

Rohini Gupta Ghasi*

Department of of Radiodiagnosis, VMMC & Safdarjung Hospital, New Delhi, India

Received: 24 November 2018
Accepted: 30 November 2018

***Correspondence:**
Dr. Rohini Gupta Ghasi,
E-mail: rohini1912@gmail.com

ABSTRACT

Background: To evaluate chest radiographic patterns in neonatal respiratory distress using a predesigned performa and algorithm and to correlate results with the clinical diagnosis.
Methods: A retrospective review was done of bedside chest radiographs acquired over a month for respiratory distress from the neonatal intensive care unit. The radiographs were systematically evaluated according to a predesigned performa and algorithm. A presumptive radiographic diagnosis was assigned to each patient based on the combination of radiographic features. Radiographic diagnosis was compared with the clinical diagnosis. The most important diagnostic features were outlined.
Results: The radiographic diagnosis correlated with clinical diagnosis in 93.3% of cases. Most common radiographic feature was pulmonary air space opacity (n=21). Air space opacity without any mediastinal shift in absence of any compensatory factors was a reliable diagnostic feature for pneumonic consolidation, which was the most common diagnosis (n=10). Bilateral granular lung fields were a specific indicator of respiratory distress syndrome. Flattening of domes of diaphragm was the most frequent feature for hyperinflation. Bilateral hyperinflation could be accurately used to diagnose bronchiolitis in all but one case (n=4/5). Pleural complications were accurately diagnosed.
Conclusions: Systematic evaluation of neonatal chest radiographic patterns of disease has a high diagnostic accuracy.

Keywords: Bronchiolitis, Chest radiograph, Neonatal respiratory distress, Respiratory distress syndrome

INTRODUCTION

Respiratory distress in the newborn is recognized as one or more signs of increased work of breathing, such as tachypnea, nasal flaring, chest retractions, or grunting.[1] Differential diagnosis includes pulmonary as well as non pulmonary causes like airway obstruction, chest wall abnormality, cardiovascular, neuromuscular or metabolic diseases.[2] Chest radiographs are the mainstay imaging modality in this scenario. Ultrasound, although available for bedside evaluation and free of ionizing radiation, is mainly limited to pleural conditions, echocardiography and lobar consolidations reaching the pleural surface. Owing to high radiation exposure, CT scan is reserved for specific indications like vascular loops, mediastinal masses or presurgical evaluation of congenital anomalies.[3]

In the era of declining familiarity with conventional radiography, the challenges of neonatal radiograph interpretation are rather overwhelming. It may be a reasonable approach to design a performa of predefined radiological features and an algorithm with core differentiating points. This could be used by radiologists and neonatal intensivists alike to distinguish between the important medical and surgical conditions causing neonatal respiratory distress.

METHODS

A retrospective review of chest radiographs referred from the neonatal intensive care unit for evaluation of respiratory distress over a period of 30 days from November 2016 to December 2016 was done. Bedside radiographs had been obtained using Allengers MARS-15 portable radiography machine using computed radiography. The radiographs had been acquired after taking due precautions needed for neonatal radiography including centring, inspiration, avoiding patient movement and proper collimation. The radiographs were reviewed on AGFA CR workstation by a single observer with over 15 years of experience in diagnostic radiology. The observer was blinded to the clinical details. The gestational age at birth, or any other clinical details were not known to the observer at the time of radiograph evaluation. The patient identification and demographic details were removed at the time of assessment. The images were viewed in the "editing" mode in a single image layout. Zoom, Pan, window alteration, invert tool were used to assist in the interpretation. Radiographs of a total of 45 neonates were available. We excluded patients with upper respiratory, chest wall, metabolic or neuromuscular causes. Only those patients where a minimum of three serial radiographs were available to confirm consistency of findings were included. Radiographs with extreme motion blur were excluded from the analysis. Finally, radiographs of 30 neonates were included in the study. A performa with predefined radiological features and a diagnostic algorithm was prepared for neonatal chest radiographic interpretation. The performa is given in Table in the appendix. The algorithm for reaching a radiographic diagnosis based in features given in performa is shown in Figure 1.

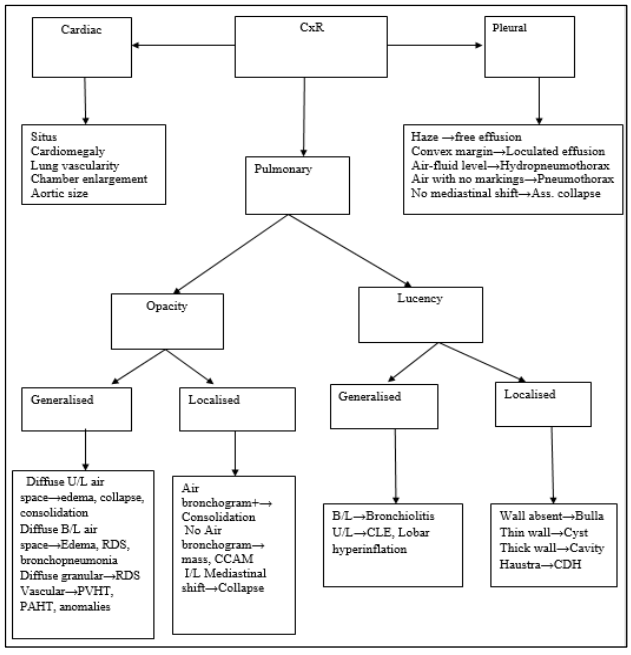

Figure 1: Diagnostic algorithm based on radiographic features in performa.

The results were tabulated in MS Excel worksheet. The numbered radiographic features found in each patient, the presumptive radiographic diagnosis derived from the algorithm was entered against each patient. The assessment was repeated after one month to test for reproducibility. The clinical details and final clinical diagnosis was then obtained from the case records. A comparative analysis of radiographic and clinical diagnosis was done. The most frequent radiographic features important for making a diagnosis of each clinical entity were noted.

RESULTS

Radiographs of 30 neonates with respiratory distress were finally included in the study. The clinical diagnoses were pneumonia (n=10 patients), bronchiolitis (n=4 patients), respiratory distress syndrome (n=5 patients), lung collapse (n=4 patients), hydropneumothorax (n=3), pleural effusion (n=1), pneumothorax (n=2), cardiac disease (n=3), congenital anomaly of lung (n=3). Combination of findings was present in 5 patients. The radiographic features, radiographic diagnosis and clinical diagnosis in each patient are given in Table 1.

Radiographic diagnosis was in sync with clinical diagnosis in all but 2 patients. There were no differences in the two assessments done at an interval of one month. In one patient with bronchiolitis, radiograph showed no abnormal findings. Radiograph in another patient was interpreted as left lobar collapse, while it was later diagnosed on CT with virtual bronchoscopy as agenesis of left lung.

Lung volume was normal in most patients. Mediastinum was central in majority of the patients, while it was deviated in 8 (26.6%) patients. Ipsilateral mediastinal shift was prevented in two patients with collapse due to compensatory hyperinflation and pleural effusion respectively. Contralateral mediastinal shift was present in 6 patients with pleural complications (n=4) and congenital lung anomalies (n=2). It was compensated by lung atelectasis in 2 patients with pleural complications.

Most common abnormality was pulmonary opacity (n=21), which was unilateral (n=11) and localised (n=10) in most cases. Presence of air bronchogram was a very specific indicator of pneumonic consolidation in the absence of volume loss (Figure 2).

Lung collpase or atelectasis was seen in four patients. Radiographic appearance was homogenous air space opacity, ususally without an air bronchogram because of mucus plugs or aspirated meconium obstructing the bronchi. Other features to distinguish collaspe from consolidation were presence of volume loss in the form of mediastinal shift or compensatory hyperinflation (Figure 3).

Table 1: Radiographic features in all patients with radiographic and clinical diagnosis.

3,4c	Normal radiograph	Bronchiolitis
3,4c,5b,7ae	Pneumonic consolidation	Lobar pneumonia
3,4b.9c	Pneumothorax	MAS with Pneumothorax
3,4c,5a,7ae	Pneumonic consolidation	Lobar pneumonia
1c,4a,5b,7af	Collapse	Resorptive collapse
3,4c,5cd,7ai	RDS	RDS
3,4c,5a,7ae	Pneumonic consolidation	Lobar pneumonia
1ab,4c	Bronchiolitis	Bronchiolitis
3,4c,5a,7ae	Pneumonic consolidation	Lobar pneumonia
3,4c,5a,7ae	Pneumonic consolidation	Lobar pneumonia
1ab,4c,5c,7d	Bronchiolitis	Bronchiolitis
2,4c,5cd,7aij	RDS	RDS
3,4c,5ab,7ae	Pneumonic consolidation	Lobar pneumonia
3,4c,5cd,7ai	RDS	RDS
3,4b,6ad	CCAM	CCAM
5c,7aj	RDS	RDS
1ab,4c,5c,7b, 8abde	R→L intracardiac shunt, PAHT	VSD Pulmonary artery HT
4c,7af,9c	Hydropneumothorax	Hydrpneumothorax
4b,7af,9c	Hydropneumothorax	Hydropneumothorax
1a,4c,5c7d	Bronchiolitis	Bronchiolitis
3,4c,8a	Cardiomegaly	Cardiomegaly
3,4b,5bd,7af, 9b	Pneumonic consolidation with pneumothorax and collapse	MAS with pneumonia, pneumothorax
3,4c,5ab,7af, 9a	Pleural effusion with collapse	Pleural effusion with collapse
3,4b,5bd,6a, 7ae,7l	CDH with C/L pneumonic consolidation	CDH with C/L bronchopneumonia
1a,4c,5ab,7af	Lobar collapse with compensatory hyperinflation	Collapse Right upper lobe
3,4c,5ab,7ae	Pneumonic consolidation	Lobar pneumonia
3,4c,5ab,7ae, 8ab	R→L intracardiac shunt with pneumonic consolidation	VSD with pneumonia
1a,4c,5ab,7a e	Pneumonic consolidation	Aspiration pneumonia associated duodenal stenosis
1abc, 4a, 5b, 6b, 7af	Collapse left lung	Agenesis lung
3,4b9b	Pneumothorax	Pneumothorax post road traffic accident

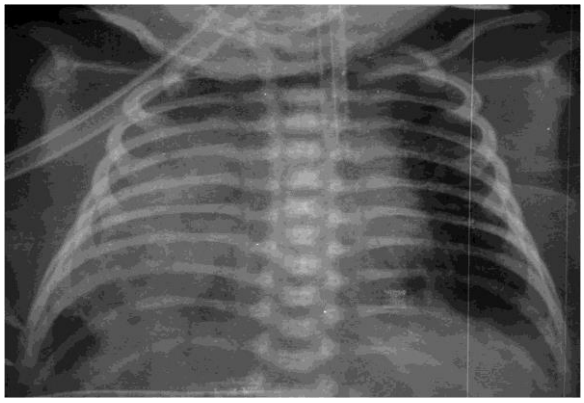

Figure 2: Unilateral right air space opacity seen with air bronchogram suggestive of pneumonic consolidation.

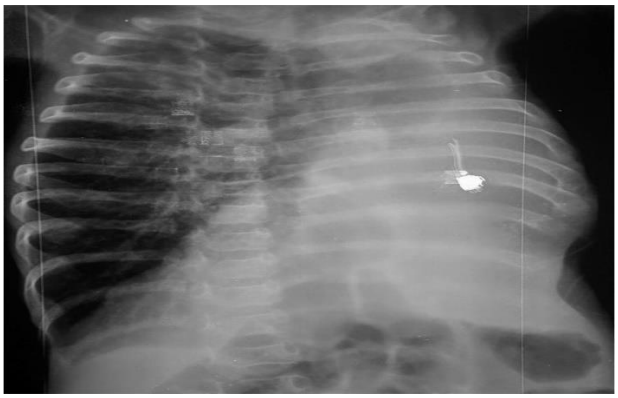

Figure 3: Unilateral left air space opacity with no air bronchogram.

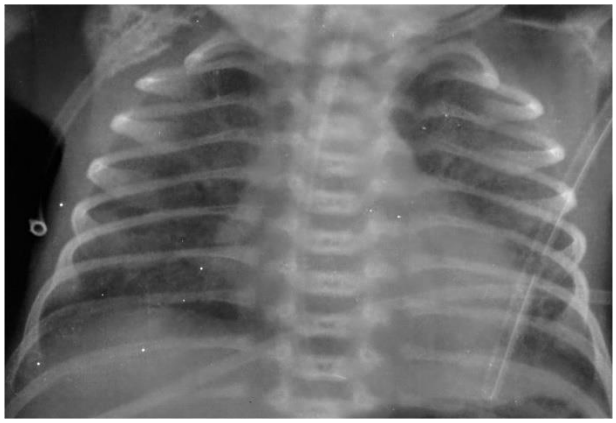

Figure 4: Bilateral diffuse coarse lung granularity in respiratory distress syndrome.

Respiratory distress syndrome was accurately diagnosed by the presence of diffuse lung granularity (Figure 4). Complete white out lung was observed in 2 patients.

Hyperinflation was present in 8 patients. Flattening of domes of diaphragm was the most sensitive feature for hyperinflation. Hyperinflation was present in all but one patient of bronchiolitis. Bilateral hyperinflation was a

very specific indicator of neonatal bronchiolitis (Figure 5). Linear atelectatic opacities could also be seen due to mucus plugging.

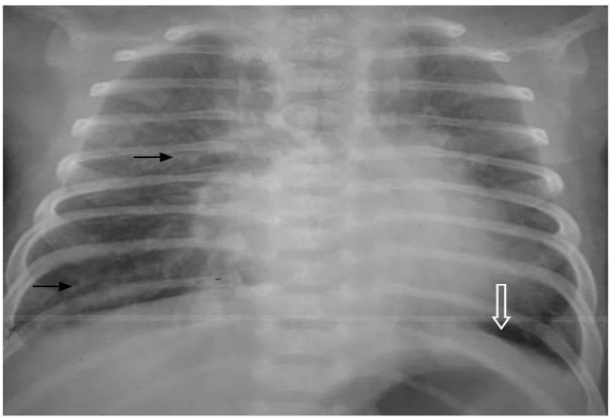

Figure 5: Bilateral hyperinflated lung fields indicated by flattened domes lying below 6th ribs (open arrow). Bilateral linear atelectatic changes are also seen (arrow).

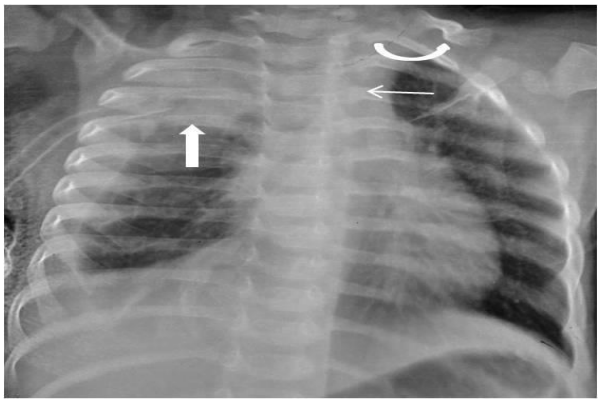

The tracheal shift (thin arrow) is in proportion to rotation (curved arrow) indicating no mediastinal shift. Opacity in right upper lobe (thick arrow) is associated collapse.

Figure 6: Right pleural effusion is seen as a homogenous extraparenchymal opacity forming obtuse angles with lung.

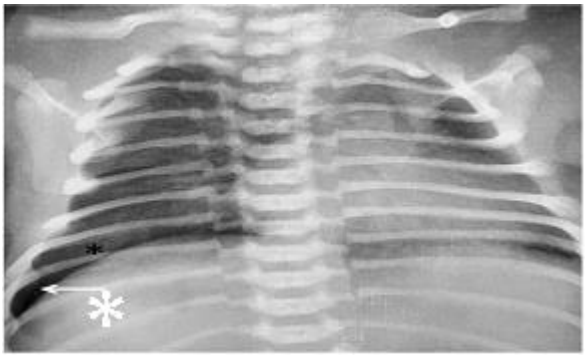

Figure 7: Right pneumothorax is seen as extrapulmonary lucency (arrow) separate from lung parenchyma which is not collapsed and shows normal lung markings (*).

Pleural complications could be diagnosed correctly in most cases by the presence of extraparenchymal opacity, often with obtuse angle with lung. Contralateral mediastinal shift was mostly present and a lack of mediastinal shift would prompt a search for associated collapse (Figure 6). Ellis curve was normally not seen in supine neonatal radiographs. Free effusion could also be seen as ill defined haze due to thin film of pleural fim in supine position.

However, since we did not conduct any cross-sectional imaging diagnosis for confirmation, small pleural effusions may not have been revealed by radiographs or clinical examination alone. However, these would generally not alter the critical care management. Pneumothorax was detected in 2 patients as extrapulmonary air with no vascular markings (Figure 7).

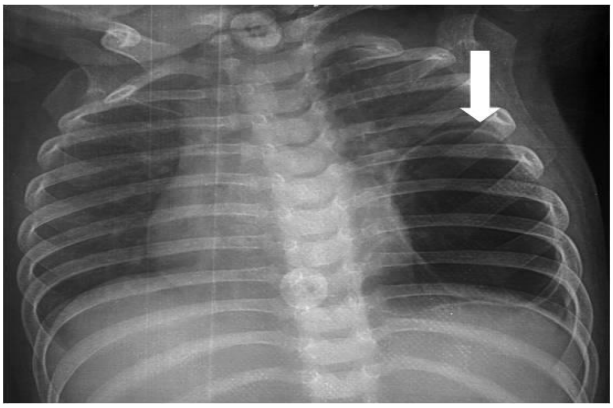

Figure 8: Multiple focal lucencies with thin walls are seen in left lower lobe (arrow) in a patient with CCAM. Note the contralateral mediastinal shift.

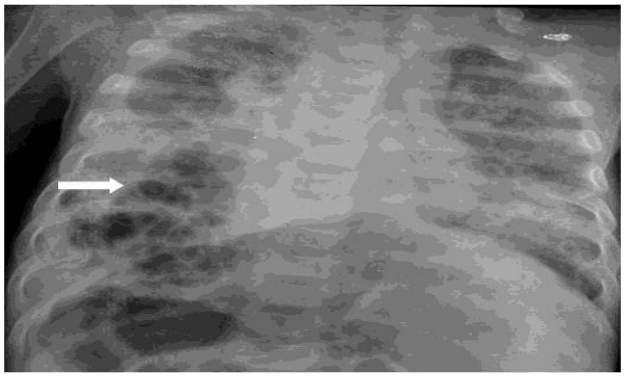

Figure 9: Presence of clustered focal lucencies with haustrations (arrow) in right lower zone and right hypochondrium in a patient with CDH. Note mediastinal shift and contralateral pneumonia.

Congenital lung anomalies were present in three patients and could be diagnosed radiographically in two patients. CCAM was seen as multiple focal lucent areas in lung with well defined thin walls (Figure 8).

CDH was an important clincial differential among congenital anomalies and was seen in one patient in our study. A cluster of focal lucencies was seen in right hemithorax with medistinal shift to opposite side. On careful inspection haustral markings could be identified amongst the focal lucencies indicating bowel in thoracic cavity (Figure 9).

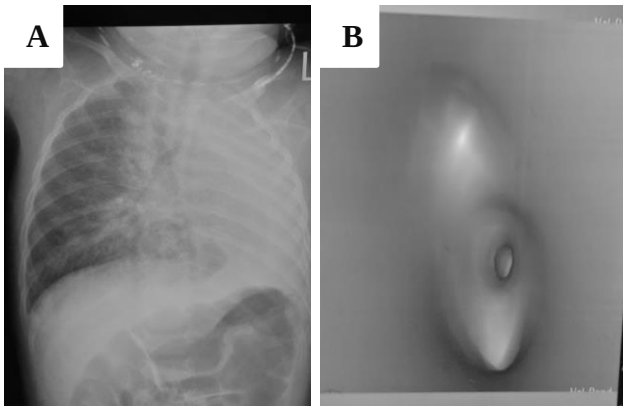

Figure 10: A) Radiograph misdiagnosed as left lung collapse due to unilateral hemithoracic opacity with ipsilateral marked mediastinal shift. B) CT virtual bronchogram through the carina shows lack of left main bronchus (arrow) suggestive of agenesis left lung.

One patient was misdiagnosed on radiograph as pulmonary collapse. There was presence of unilateral opaque left hemithorax with marked ipsilateral mediastinal shift. No air bronchogram was seen. As per the performa and algorithm, a diagnosis of collapse left lung was given. However, since there was no improvement on conservative management, a CT with virtual bronchoscopy was done, which revealed absence of left main bronchus. A diagnosis of agenesis of left lung was finally made (Figure 10A and B).

Figure 11: Cardiomegaly with right ventricular type of apex (thick arrow) with enlarged pulmonary artery (thin arrow) and plethoric lung fields in a patient with VSD.

Cardiac abnormalities were seen in three patients. Cause of cardiomegaly could not be ascertained in one patient, while presence of right ventricular enlargement and pulmonary hypertension allowed the diagnosis of right to left shunt in one patient (Figure 11). Right to left shunt was similarly diagnosed in another patient with right ventricular enlargement and normal aortic size.

DISCUSSION

The minimum gestational age and birth weight for neonatal survival has been continuously receding as an outcome of improves neonatal intensive care. Thoracic abnormalities are a major contributor to neonatal morbidity and mortality.[4] Bedside radiographs are the most useful and feasible modality in the neonatal intensive care unit. Bedside ultrasound is also widely available, but due to inherent limitations of the thoracic anatomy, is mainly used for diagnosis and management of pleural disease. Computed tomography and other sophisticated modalities are reserved for special cases where surgical intervention may be required.[3]

However, acquiring a good quality neonatal chest radiograph is a daunting task because of problems of rotation, improper centring, tachypnea, motion blur and proper end inspiratory timing.[5,6] A learning curve exists for interpretation of neonatal chest radiographs because of differences in chest anatomy and physiology in the neonate and adult.[7] A recent study indicated a difference of about 34% in the diagnostic interpretation between pediatric intensivists and radiologists, most important areas being air leaks and pulmonary opacity categorization.[8]

This study is an endeavour to design a performa and a simplified algorithm for the use of pediatric intensivists and young radiologists.

Radiographic diagnosis was correlated with clinical diagnosis in 93.3% cases. One case of bronchiolitis did not reveal any abnormality on chest radiograph, although clinically bronchial wheezing was present. Another case of lung agenesis was misdiagnosed as collapse.

Pneumonic consolidation was the most common diagnosis (n=10), either alone or in combination with cardiac or congenital anomalies. The commonly described appearance of neonatal pneumonia is patchy air space opacity with air bronchogram, which may be bilateral.[9] Frank consolidation is known to be less common.[2] Patchy distribution of opacities and pleural effusion, if present, allow reliable differentiation from RDS.[3,4,10] In our study, frank consolidation was frequently present. It was accurately diagnosed on the basis of localised pulmonary air space opacity with presence of air bronchogram and no signs of lung volume loss.[11] Lobar or pneumonic collapse was present in 4 patients and was seen as localised air space opacity with

mediastinal shift or compensatory mechanisms like hyperinflation.

Respiratory distress syndrome of the newborn was present in 5 patients. The classic appearance of RDS is diffuse homogenous granular opacities with low lung volumes.[2] This may be altered by administration of exogenous surfactant or mechanical ventilation. The appearance may overlap with neonatal pneumonia or meconium aspiration.[3] Coarse granular lungs were the most common feature, while complete "white out" lung was also present in two patients. Early RDS with fine lung granularity was not present in any case in this study, probably because the sample population was derived from neonatal intensive care unit of a tertiary hospital, leading to severe nature of lung abnormalities in most cases. One of the cases of RDS in our study had developed pneumothorax, possible as a complication of mechanical ventilation.

Pleural effusion as well as pneumothorax and hydropneumothorax were clinically correlated in all patients. However, small effusions and air leaks may not reveal themselves clinically and may have been missed on the radiograph. Our study had the limitation that we used only clinical correlation for confirmation of diagnosis. However, since the purpose of the study is management oriented diagnosis of neonatal thoracic pathologies, small pleural pathologies may not make a difference to the overall results.

Cardiac abnormalities were present in 3 patients in this study. A systematic evaluation of chest radiograph for cardiac disease has been described in literature.[12] We similarly developed an approach to observe the situs, cardiac and chamber size and position, mediastinal contour for great vessels and lung vascularity. A diagnosis of shunt direction and pulmonary arterial hypertension could be made radiographically. However, since the sample size was small and we did not perform any echocardiographic correlation, we cannot conclude that this is the overall accuracy of chest radiograph in neonatal cardiac disease. We can only infer that overt cardiac disease leading to significant hemodynamic changes can be reliably detected.

Congenital lung anomalies were present in three patients. Two patients showed typical features of CCAM and CDH and were diagnosed easily on chest radiograph. One patient with lung agenesis was misdiagnosed as lung collapse. However, since these cases are surgically managed, advanced imaging techniques are required in more complex cases.

There were several limitations in our study. We developed a simplified algorithm for basic use by intensivists and young resident radiologists. The radiographic picture may be complicated by mechanical ventilation, co-existence of multiple pathologies, surfactant treatment, etc. We compared our results with clinical records but did not carry out specific investigations because it was a retrospective study.

To the best of our knowledge, various authors have described the role of chest radiography in neonatal respiratory distress. Many authors have also given systematic approach.[4,5] However, we devised an exhaustive performa and detailed algorithm to allow for diagnosis of common conditions and identify the features crucial to management decisions.

CONCLUSION

Chest radiography has an indispensable role in neonatal respiratory distress. Systematic approach can help in easy interpretation and minimize errors in diagnosis. Our study indicates that radiographic differential diagnosis of common causes of neonatal respiratory distress can be simplified using a systematic approach. Usual causes like pneumonia, respiratory distress syndrome, collapse, pleural complications, cardiac diseases and common congenital anomalies can be confidently diagnosed.

Funding: No funding sources
Conflict of interest: None declared
Ethical approval: The study was approved by the Institutional Ethics Committee

REFERENCES

1. Reuter S, Moser C, Baack M. Respiratory distress in the newborn. Pediatrics in review. 2014;35:417-29.
2. Pramanik AK, Rangaswamy N, Gates T. Neonatal respiratory distress: A practical approach to its diagnosis and management. Pediatr Clin north Am. 2015;62:453-69.
3. Liszewski MC, Stanescu AL, Phillips GS, Lee EY. Respiratory Distress in Neonates. Radiol Clin North Am. 2017;55:629-44.
4. Lobo L. The neonatal chest. Eur J Radiol. 2006;60:152-8.
5. Alford BA, McIlhenny J. An approach to asymmetric neonatal chest radiograph. Radiol Clin North Am. 1999;37:1079-92.
6. Pederson CCE, Hardy M, Blankholm AD. An Evaluation of Image Acquisition Techniques, Radiographic Practice, and Technical Quality in Neonatal Chest Radiography. J Med Imaging Radiat Sci. 2018;49:257-64.
7. Menashe SL, Iyer RL, Parisi MT, Otto RK, Stanescu AL. Pediatric chest radiographs: common and less common errors. AJR. 2016;207:903-11.
8. Fink AZ, Levin TL, Blumfield E, Nemerofsky SL, Liszweski MC, George K, et al. Discrepancies in radiographic interpretation between pediatric radiologists and pediatric intensivists in the pediatric or neonatal intensive care unit. J Am Coll Radiol. 2018;15:1580-6.

9. Edwards MO, Kotecha SJ, Kotecha S. Respiratory distress of the term newborn infant. Pediatr Resp Rev. 2013;14:29-37.
10. Suprenant S, Coghlan MA. Respiratory distress in the newborn: an approach for the emergency care provider. Clin Pedia Emerg Med. 2016;17:113-21.
11. Haney PJ, Bohlman M, Sun CCJ. Radiographic findings in neonatal pneumonia. AJR. 1984;143:23-6.
12. Schweigmann G, Gassner L, Maurer K. Imaging the neonatal heart-Essentials for the radiologist. Eur J Radiol. 2006;60:159-70.

Cite this article as: Ghasi RG. Decoding neonatal chest radiographic patterns of disease: retrospective analysis from a tertiary care hospital. Int J Res Med Sci 2019;7:77-84.

APPENDIX

Performa with numbered radiographic features from 1a to 9c
1. Hyperinflation
1. Flattening of domes of diaphragm
2. Dome of diaphragm below 6th interspace
3. Lung herniation
2. Low lung volumes
3. Normal lung volumes
4. Mediastinal shift
a. Ipsilateral to the side of abnormal lung pattern
b. Contralateral to the side of abnormal lung pattern
c. Central mediastinum
5. Lung opacity
a. Focal opacity
b. Unilateral
c. Bilateral
d. Diffuse
6. Lung lucency
a. Focal lucency
b. Unilateral diffuse
c. Bilateral diffuse
d. Cyst with thin walls
7. Type of lung opacity
a. Air space
b. Vascular
c. Peribonchial cuffing
d. Linear atelectasis
e. Consolidation with air bronchogram
f. Collapse
g. Reticulonodular pattern
h. Fine granularity
i. Coarse granularity
j. White out lungs
k. Cavity with air fluid levels
l. Haustra or mucosal folds
8. Cardiac anomaly
a. Cardiomegaly
b. Specific chamber enlargement
c. Pulmonary venous hypertension
d. Pulmonary arterial hypertension
e. Abnormal mediastinal contour
9. Pleural complication
a. Pleural effusion
b. Pneumothorax
c. Hydropneumothorax